Engineering Structures 292 (2023) 116516

Contents lists available at ScienceDirect

Engineering Structures

journal homepage: www.elsevier.com/locate/engstruct

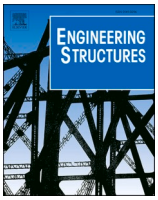

Flexural strengthening of RC beams using GFRP grid bonded with sprayed polyurea

Piyong Yu [a,*], Pedro Silva [b], Antonio Nanni [c]

[a] Faculty of Architecture,Civil and Transportation Engineering, Beijing University of Technology, 100 PingLe Yuan, Chaoyang District, Beijing, China
[b] Department of Civil and Environmental Engineering, George Washington University, USA
[c] Department of Civil and Architectural Engineering, University of Miami, USA

ARTICLE INFO

Keywords:
GFRP
Grid
Polyurea
Impregnation
Reinforced concrete
Strengthening

ABSTRACT

Flexural strengthening of reinforced concrete (RC) beams with fiber reinforced polymer (FRP) was investigated in this research. The bonding agents were an epoxy paste and a sprayed polyurea. Four RC beams were strengthened with FRP composites according to the following techniques: (a) sprayed polyurea with and without glass FRP (GFRP) grid reinforcement; (b) manual layup with one GFRP grid; and (c) manual layup with one GFRP sheet. Experimental results clearly shows that flexural strengthening with polyurea technique is an effective scheme. Other than fast setting, the major advantages of using polyurea over other organic or inorganic matrices are as follows: (a) no slippage of the FRP grid from the polyurea or cracking of the polyurea occurred during the tensile test; (b) no debonding of the polyurea system from strengthened RC beams was observed during the bending test. Application of the polyurea system, key experimental results, and comparison with findings from other research programs reported in literature are presented in this paper.

1. Introduction

The use of fiber reinforced polymer (FRP) composites is now a widely-accepted solution for the strengthening of reinforced concrete (RC) members. FRP systems, which are typically made of carbon, glass, PBO, basalt, or aramid fibers, offer suitable combination of mechanical properties for RC strengthening applications, which include: (1) low-weight, (2) immunity to corrosion; and (3) excellent mechanical strength and stiffness in the fiber direction. In addition, FRP systems can be custom tailored and are easy to handle and install, producing effective strengthening solutions that are economical [1–4]. However, some drawbacks exist with the use of externally bonded FRP, including: poor performance of the polymer matrix at high temperature or in presence of fire, difficulty to bond on a wet concrete substrate, and lack of permeability when the substrate necessitates to release moisture such as in historical structures [5,6]. Therefore, alternative strengthening systems with cement-based matrix, known as fabric reinforced cementitious matrix (FRCM) have been studied in recent years [6–8]. FRCM is also called textile reinforced mortar (TRM) or engineered cementitious composites (ECC).

Direct tensile test employing clevis grid or clamping grid system has been conducted to characterize the material properties of FRCM composites. The experimental stress–strain response varied according to the properties of the different constituents of the composite and followed a bi-linear or tri-linear behavior [9–12]. The relationship may generally be divided in two phases: (1) before cracking, the tensile load was carried by the matrix and the fabric, and (2) after cracking, the load is gradually transferred to the textile reinforcement. As the ultimate strain of the cementitious matrix is generally smaller than that of the fabric, the matrix fails long before the reinforcement reaches the tensile strength [13].

Carozzi and Poggi [10] reported that the ultimate strain of FRCM at failure was lower than that of fabric measured in the tensile test. Orosz et al. [5] found that the rupture strain of the fabric in strengthening of RC beams with FRCM was around 50% of the ultimate strain recorded from coupon tests in tension. Generally in strengthening RC beams with different fibers and inorganic matrices, failure mainly is due to debonding of the strengthening system at a strain of the fibers or fabric that is much smaller than their ultimate strain [6,14,15].

In order to improve the bond between filaments inside yarns and between mortar matrix and yarns, the dry fabric can be impregnated with an organic resin to create an FRP grid before the mortar matrix application [5,9,16]. It was reported that the tensile strength and shear bond strength of FRCM were increased after the fabric was coated or

* Corresponding author at: College of Civil and Architectural Engineering, Beijing University of Technology, 100 PingLe Yuan, Chaoyang District, Beijing, China.
E-mail addresses: yupy@bjut.edu (P. Yu), silvap@gwu.edu (P. Silva), nanni@miami.edu (A. Nanni).

https://doi.org/10.1016/j.engstruct.2023.116516
Received 8 September 2022; Received in revised form 12 May 2023; Accepted 19 June 2023
Available online 4 July 2023

impregnated [17]. A few research programs have been conducted to investigate the flexural performance of RC beams retrofitted with impregnated FRP grid. Zheng et al. [18] tested five beams strengthened with FRP grid reinforced ECC and observed rupture of the grid and partial debonding of the grid layer from the concrete substrate. Yang et al. [19] studied RC beams strengthened with FRCM and observed failure modes included local debonding, rupture of the FRP grid, separation of the grid and shear-crack induced debonding. Guo et al.[20] reported four-point bending test results of RC beams strengthened with carbon FRP (CFRP) grid reinforced mortar and observed CFRP debonding and rupture of the grid. Zheng et al. [21] studied corrosion-damaged RC beams strengthened with FRP grid-reinforced ECC matrix composites and observed grid rupture, debonding of the composites and others. These researches clearly demonstrated that the application of impregnated FRP grid is effective in increasing the flexural strength of RC beams.

A new FRP strengthening scheme that combines an organic matrix (typical of FRP manual lay-up) with pre impregnated FRP grid (typical of FRCM/ECC) was investigated in this research. It consists of a fast-setting polyurea matrix that was sprayed over a glass FRP (GFRP) grid to form the composite. Polyurea is a unique class of polymers and combines good application properties, such as rapid cure and insensitivity to substrate moisture, with equally good physical properties, such as high hardness, flexibility, tear and tensile strength [22,23]. Sprayed polyurea coating of deteriorated concrete surfaces has been a commonly-used technique for corrosion prevention of the exposed internal steel reinforcement.

The sprayed polyurea has been used in structural strengthening recently. It was reported that the flexural and shear capacity and ductility of the RC beams strengthened with polyurea coating system were improved when compared with unstrengthened beams [24,25]. It was found that flexural strength and ductility of RC slabs were increased after retrofitted with sprayed polyurea [26]. However, to the best knowledge of the authors, these references [22–26] represent the current major state of publicly available literature devoted to the strengthening of flexural members with the sprayed polyurea. Certainly, further research is needed before the system can be widely applied in increasing the structural performance of RC members. In this research, the properties of the polyurea system were first studied through direct tensile test. Then RC beams strengthened with sprayed polyurea and polyurea-impregnated GFRP grid were investigated as well as RC beams retrofitted by manual lay-up using an epoxy-impregnated GFRP grid and epoxy-impregnated GFRP sheet. These two manual lay-up schemes provided a means for direct comparison with the sprayed polyurea system. The application of polyurea and detailed experimental work together with results from literature related to similar systems were presented in this paper.

2. Experimental test program

2.1. Direct tensile test of polyurea system

The GFRP grid was made with glass fiber mesh coated with epoxy and in the form of individual longitudinal fiber yarns connected to each other by transverse yarns of smaller size (Fig. 1). The average cross-sectional area of one longitudinal yarn was 4.3 mm^2 and the spacing between yarns was 11.3 mm. In order to achieve loading uniformity the GFRP grid was further impregnated with resin in the lab for tensile test. Each coupon had four longitudinal yarns and averaged width of 51.5 mm during the tensile test.

The unreinforced-polyurea coupons were prepared by spraying polyurea on a plastic sheet placed on a horizontal flat surface and then the coupons were cut from the sprayed polyurea. The average width and thickness of four coupons were 47.32 mm and 5.3 mm, respectively.

For the production of polyurea-GFRP coupon, the polyurea was first sprayed onto a flat surface and then one ply of GFRP grid was laid upon the matrix with additional polyurea sprayed over the grid. The averaged width and thickness of the three grid reinforced polyurea coupons were 51.63 mm and 7.19 mm, respectively. The volume ratio of the GFRP grid was approximately 5.3% of the overall cross-section, with polyurea constituting the remaining fraction.

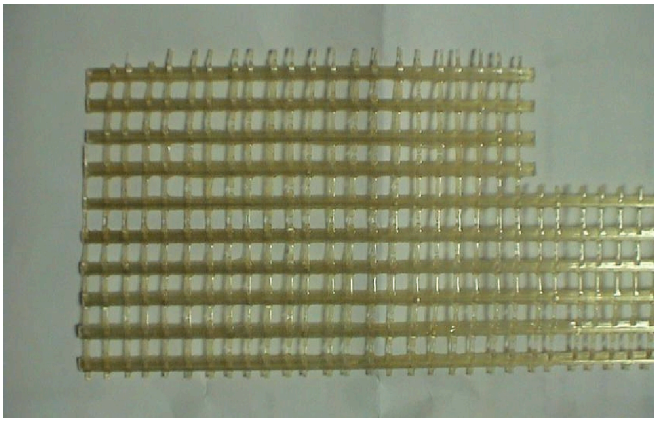

Fig. 1. The GFRP grid.

The tensile test was carried out with universal testing machine with clamping grid system. The plain GFRP grid, polyurea and GFRP grid reinforced polyurea coupons were uniaxially loaded to failure with cross-head displacement rate of 1.5 mm/min according to ASTM D3039 [27].

2.2. Test setup and instrumentation of RC beams

Four RC beams were strengthened according to the schemes shown in Table 1. As shown in Fig. 2b, the cross-sectional dimensions were 203 × 279 mm^2. Longitudinal reinforcement in the tension and the compression zone consisted of 2-D16 and 2-D10 steel bars, respectively. All beams were tested under a symmetric 4-point static loading system, as shown in Fig. 2a. Two heavy-duty rollers were used to support the beams with a span of 2.13 m and two other rollers were used at the point loads. These rollers were placed at equal distances along the length of the beams, leading to a shear span-to-depth ratio of approximately 2.80. Based on this ratio, no arching effect was expected to occur during testing of these beams [28]. One load cell was placed between the hydraulic jack and the supporting steel beam to measure the applied load, and two strain transducers were installed on either side of the beams to record the midspan defection (Fig. 2a). In the retrofitted beams, five strain gauges were attached to the external strengthening systems.

2.3. Test matrix and strengthening schemes of RC beams

As shown in Table 1, Beam A was used as the control element without strengthening. Beams B and C were strengthened with polyurea and GFRP grid bonded with polyurea, respectively. Beam D was retrofitted with the same amount of GFRP grid installed by manual lay-up. Prior to strengthening, the concrete surface of the strengthened beams was roughened with a grinder to expose the aggregates according to ACI 546 [29] and ICRI [30].

For Beams B and C, the area surrounding the beams was properly protected using thick plastic sheets before spraying the polyurea, which cured within minutes after spraying. For Beam C as shown in Fig. 3 that a layer of GFRP grid was placed over the first layer of polyurea and an additional layer of polyurea was sprayed immediately over the GFRP grid until it was completely covered. In Beams B and C the polyurea layer was maintained to approximately 7 mm in thickness.

For Beams D and E the strengthening scheme employed the traditional manual lay-up technique. From an installation point of view, the sprayed polyurea technique was significantly less time consuming when

Table 1
Text matrix and comparison of recorded midspan strains at failure.

Beam	Strengthening scheme	Failure mode	Fabric area A_f (mm^2)	Tensile Reinforcing Steel ($\mu\varepsilon$)	Polyurea or FRP ($\mu\varepsilon$)	Polyurea or FRP strain ratio
A	NA	Steel yielding followed by concrete crushing	–	15,000 **	–	–
B	Unreinforced polyurea	Steel yielding followed by concrete crushing	1422#	15,000 **	15,000 **	–
C	GFRP grid reinforced polyurea	GFRP grid rupture followed by concrete crushing	77	11,800	13,300	0.57
D	Manual lay-up GFRP grid	GFRP grid rupture followed by debonding	77	12,900	15,000 **	–
E	Manual lay-up GFRP sheet	GFRP sheet rupture followed by debonding	129	3,400 *	12,000	0.52

** The capacity of the strain gage was 15,000 ($\mu\varepsilon$), so the actual strain may have exceeded this value.
* The measured strain dropped before the beam reached the ultimate condition. #Cross-sectional area of polyurea.

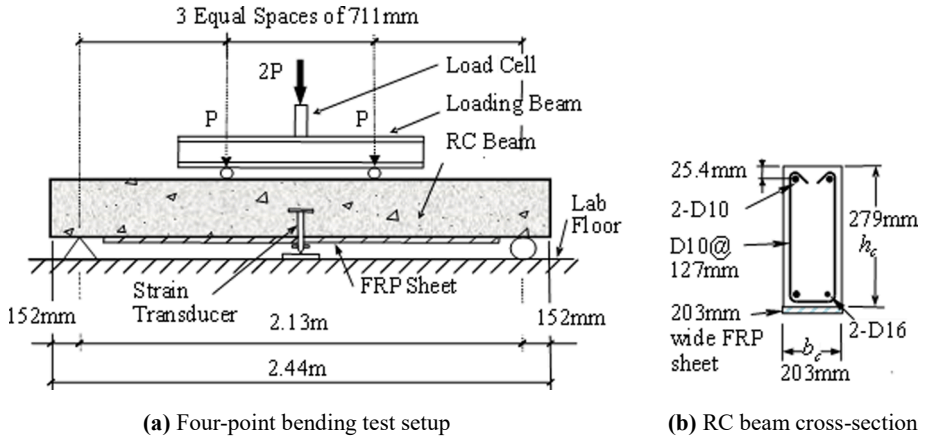

(a) Four-point bending test setup **(b)** RC beam cross-section

Fig. 2. Test setup and beam cross-section.

(a) Applying the GFRP grid **(b)** spraying of polyurea

Fig. 3. Application of GFRP grid over polyurea in beam C.

compared to the manual lay-up technique. However, a disadvantage of this system is that it requires the assistance of a qualified technician for obtaining a uniform thickness and consistency of resin distribution.

3. Experimental results and theoretical analysis

3.1. Material properties

Impregnated GFRP grid: The rupture of grid was brittle and occurred consecutively. As shown in Fig. 4 the stress–strain relationship is elastic until ultimate condition. The averaged properties are: tensile strength 587 MPa, elastic modulus 37 GPa, and ultimate strain 1.8%.

Unreinforced Polyurea: The typical failure mode is shown in Fig. 5a and no visible cracks were observed outside of the breakage area. The averaged experimental properties are: tensile strength 7 MPa, initial elastic modulus 200 MPa, and ultimate strain 43.8%. As shown in Fig. 5 that the experimental stress–strain relationship could be divided into two phases: elastic portion and strain hardening portion, and the limit strain for elastic deformation is around 3% and greater or close to the ultimate strain of most fibers, which is usually 1–3% [12]. Therefore, it could be expected that the polyurea could deform elastically with reinforcement if used as matrix for a grid reinforced composite and no crack would happen before rupture of the grid under tension.

GFRP grid reinforced polyurea: The coupons failed due to rupture of the grid (Fig. 6). Before reaching the ultimate condition, no crack of the polyurea or slippage of grid inside the polyurea was observed. The

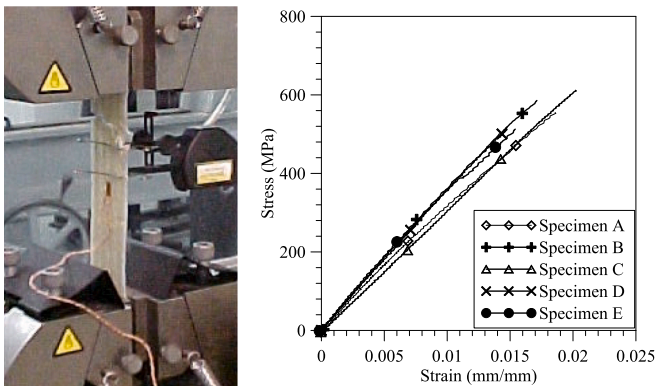

(a) failure mode **(b)** stress-strain response

Fig. 4. Tensile test of GFRP grid.

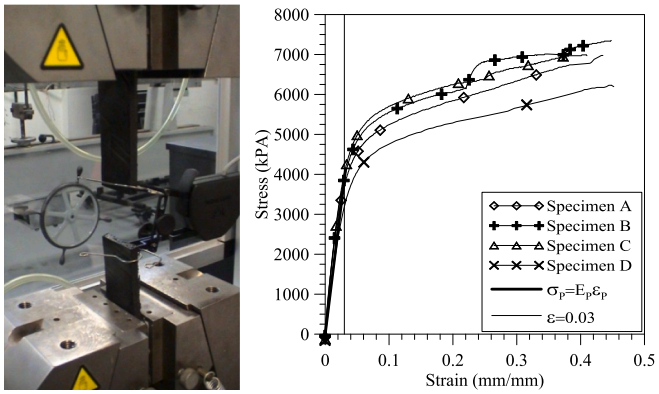

(a) failure mode **(b)** stress-strain response

Fig. 5. Tensile test of plain polyurea.

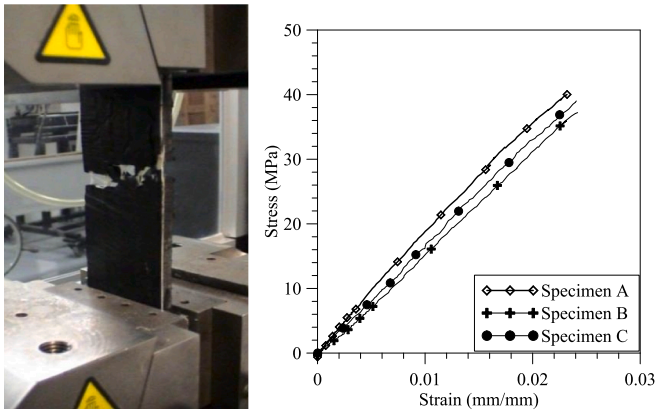

(a) failure mode **(b)** stress-strain response

Fig. 6. Tensile test of grid reinforced polyurea.

typical stress–strain behavior of FRCM [31,32] during tensile test was not observed. Based on the gross cross-section of the composites the average mechanical properties of the grid reinforced polyurea are as follows: tensile strength 39 MPa, elastic modulus 2 GPa, and the ultimate strain 2.3%. Based solely on the cross-sectional area of the GFRP grid the tensile strength is 736 MPa and the elastic modulus is 37.7 GPa. Compared with the plain grid, the rupture strain increased from 1.8% to 2.3% when polyurea was employed. It is depicted in Fig. 6b that the stress–strain relationship is nearly elastic until failure and the elastic modules can be evaluated with the following equation:

$$E_f = (1-\frac{A_g}{A_f})E_P + E_g\frac{A_g}{A_f} \quad (1)$$

Where, E_f, E_g,E_p are the elastic modulus of the composites, grid, and polyurea, respectively. A_f and A_g are the cross-sectional area of composites and the grid, respectively. Given A_g/A_f equals to 5.3%, the elastic modulus calculated per Eq. (1) is 2.15 GPa, which is slightly greater than the value of 2 GPa determined through the tensile test of the composite.

Steel bar and concrete: For the D16 steel bars, the average yield and ultimate strength was 416 MPa and 654 MPa, respectively. For the D10 steel bars, the average yield and ultimate strength was 434 MPa and 620 MPa, respectively. The experimental compressive strength of concrete was 40 MPa.

GFRP sheet: The experimental properties: tensile strength 1700 MPa, elastic modulus 83 GPa, and the ultimate breaking strain of 2.3%. The thickness of the GFRP sheet was 0.64 mm.

3.2. Theoretical and experimental response of the tested RC beams

In this section, theoretical results derived from a coupled moment–curvature computer program and nonlinear model for deformation calculations are compared against experimental results. Fig. 7 outlines a schematic of the nonlinear model in which the applied load is referred to as P (Fig. 2a and 7). Because of symmetry only half of the beam was considered in the model. The theoretical load-deformation responses were developed using the section dimensions depicted in Fig. 2b, and the material properties and the reinforcement layout depicted in Table 2. Development of the nonlinear model and detailed analysis of mid-span deflections can be found in Yu et al. [33] and for brevity they are not repeated in this paper.

Beam A: The first crack was observed at load of 15.6 kN and the beam failed as the concrete in the compression zone crushed (Fig. 8). Fig. 9 shows that the experimental deflection matched reasonably well the theoretical prediction except for the ultimate deflection. This is because concrete strains registered at ultimate may significantly exceed the strains typically used in the design of RC beams, which is 0.003 per ACI 318 [34]. In the results shown in this section all the concrete strains at ultimate were allowed to reach 0.004.

Beam B: The cracking load was 22.2 kN. Failure occurred due to concrete crushing after the tensile reinforcement yielded and no crack of polyurea was observed (Fig. 10). Compared to Beam A, a much higher number of cracks was registered and maximum crack width was lower. The recorded strain profile did not develop linearly along the span of the beam (Fig. 11).

Beam C: The cracking load was 22.2 kN. At failure, the GFRP grid reinforced polyurea ruptured at midspan, followed by crushing of concrete in the compression zone (Fig. 12). As depicted in Fig. 13, the strain profiles depict a linear variation that is in agreement with the load-deformation response, which shows a well-defined bi-linear response.

Beam D: The cracking load was 24.5 kN. The failure was caused by rupture of the GFRP grid layer in the shear-moment region and then debonding of the grid propagated towards the opposite end of the beam. At failure a small portion of concrete cover separation was caused by the

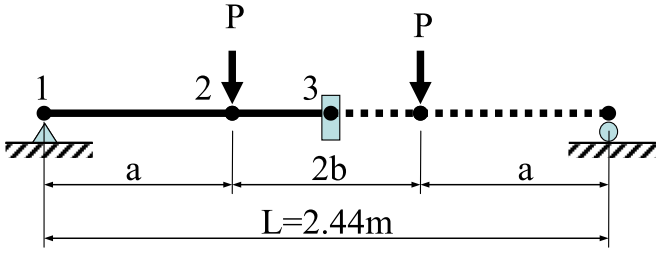

Fig. 7. Theoretical model for system evaluation.

Table 2
Comparison of experimental and theoretical results of RC beams.

Beam ID	Fabric area A_f (mm^2)	Theoretical Ultimate midspan Δ_u (mm)	Ultimate P_u (kN)	Experimental Cracking P_{cr} (kN)	Yielding P_y (kN)	P_u (kN)	Yielding midspan Δ_y (mm)	Δ_u (mm)	ΔP_u (kN)	$\frac{P_u}{A_f E_f}$	$\frac{\Delta P_u}{A_f E_f}$	Ductility index $\frac{\Delta_u}{\Delta_y}$	Bending stiffness ($kN{\cdot}m^2$)(Eq.2)
A	–	78.1	69.2	15.6	41.0	64.5	6.3	83.0	–	–	–	13.2	246
B	1422[#]	77.0	70.9	22.2	38.9	67.4	7.0	92.3	2.9	0.237	0.010	13.2	254
C	77	29.8	80.8	22.2	49.6	77.3	5.8	25.7	12.8	0.027	0.005	4.4	1012
D	77	31.9	82.8	24.5	52.4	70.8	9.0	25.4	6.3	0.025	0.002	2.8	820
E	129	19.6	92.9	26.7	60.0	83.9	7.6	20.3	19.4	0.008	0.002	2.7	1129

[#] Cross-sectional area of polyurea.

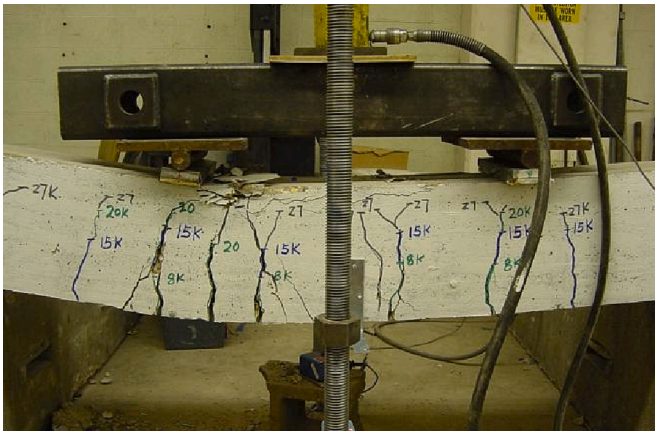

Fig. 8. Failure mode of beam A.

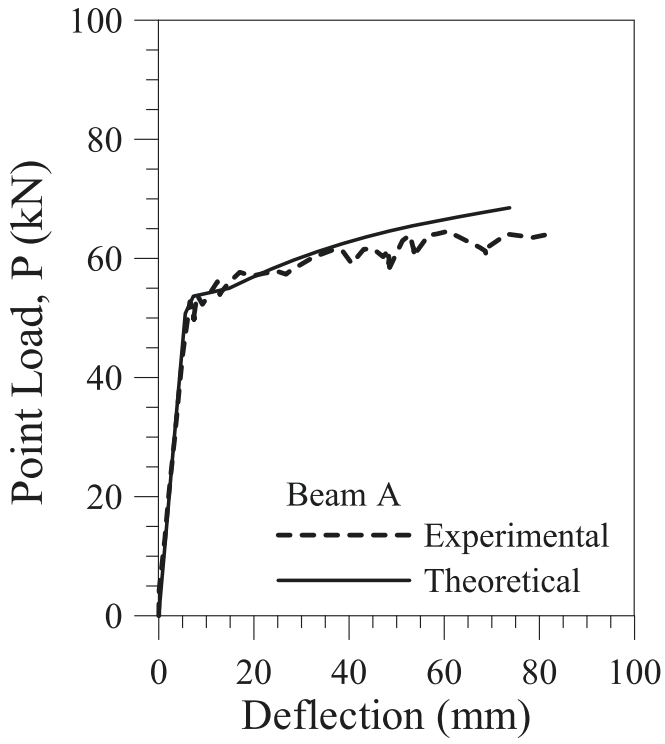

Fig. 9. Load-Deflection curves of beam A.

flexural intermediate crack near the midspan and one thin layer of concrete was attached to the strengthening layer (Fig. 14). The recorded strain depict a slight nonlinearity (Fig. 15).

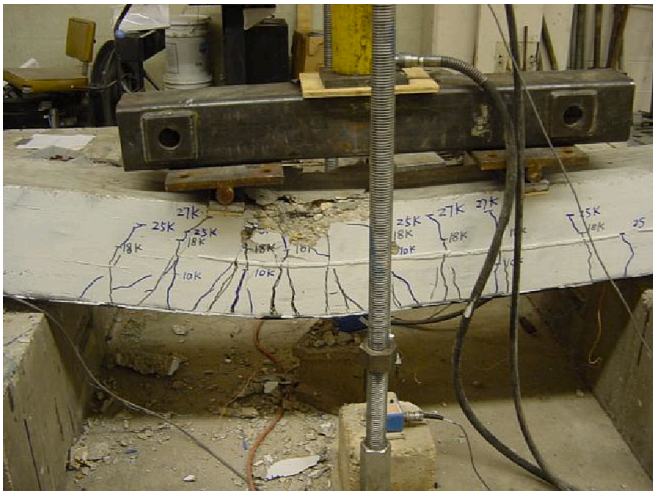

Fig. 10. Failure mode of beam B.

Beam E: The first crack was observed at midspan at load of 26.7 kN. The beam failed when the GFRP sheet partially ruptured and debonded from one end and debonding propagated towards the opposite end (Fig. 16). At failure a small portion of concrete cover separation was caused by the flexural intermediate crack in the shear moment region. A nonlinear strain profile is developed (Fig. 17).

A summary of the experimental results are depicted in Tables 1 and 2. It is important to emphasize that these tests were conducted in a four point bending test setup (see Fig. 2a). Research by Zhang et al. [35] evaluated experimentally the effect of load distribution on the behavior of Near Surface Mounted (NSM) FRP-strengthened RC beams. Zhang et al. [35] main conclusion was that load distribution impacts the beam response and the degree of this effect varies with the bond length of NSM FRP. It is thus reasonable to infer that the failure mode and ultimate loads outlined in Tables 1 and 2 are likely to differ if these beams were tested under a different loading scheme; such as, uniform distributed loads. Debonding failure of FRP reinforced RC beams, characterized by either intermediate crack (IC) debonding failure or cover delamination, are highly susceptible to high stress concentrations [36], which further indicates the need for continuing research regarding load distribution on the behavior of composite strengthened RC beams.

4. Discussion of test results of the RC beams

Table 1 indicates that for all the beams the tension reinforcements yielded before failure. It should be noted that the measured strains of the polyurea and GFRP sheet for Beams C and E at ultimate condition were between 50% – 60% of the materials' ultimate strain when the beams failed due to FRP rupture. Part of the reasons might be that the maximum strain may not be caught during the test due to the limited number of strain gauges.

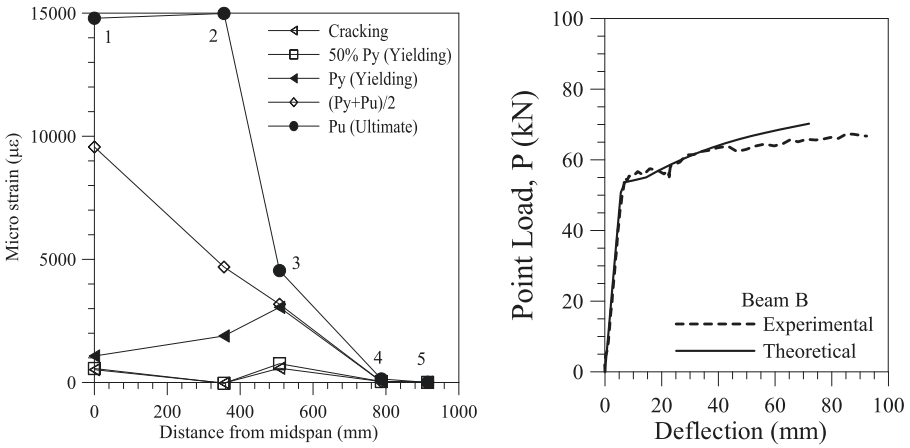

(a) Strain gage profiles **(b)** Load-Deflection curves of beam B

Fig. 11. Test results of beam B.

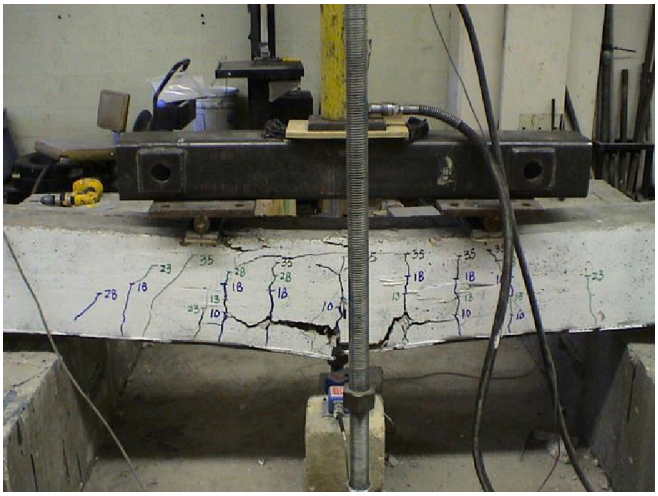

Fig. 12. Failure mode of beam C.

In Table 2, ΔP_U is the increase of the ultimate load with respect to that of Beam A. Except for Beam B, A_f and E_f are the cross-sectional area and elastic modulus of the GFRP grid or glass sheet, respectively. Although, no significant differences in midspan deflection was recorded between beams C and D, the failure load in Beam C was nearly 10% higher than that in Beam D. This change in load capacity can be directly attributed to the different failure modes as beam D failed mainly due to FRP delamination (Fig. 14) and beam C was by FRP rupture at midspan (Fig. 12). Furthermore Fig. 18 shows that application of GFRP grid could significantly increase the flexural strength of RC beam, but its contribution to the increase of secant stiffness is negligible.

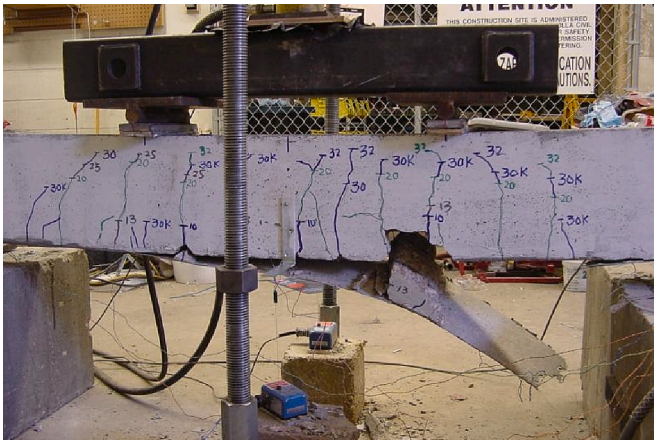

Fig. 14. Failure mode of beam D.

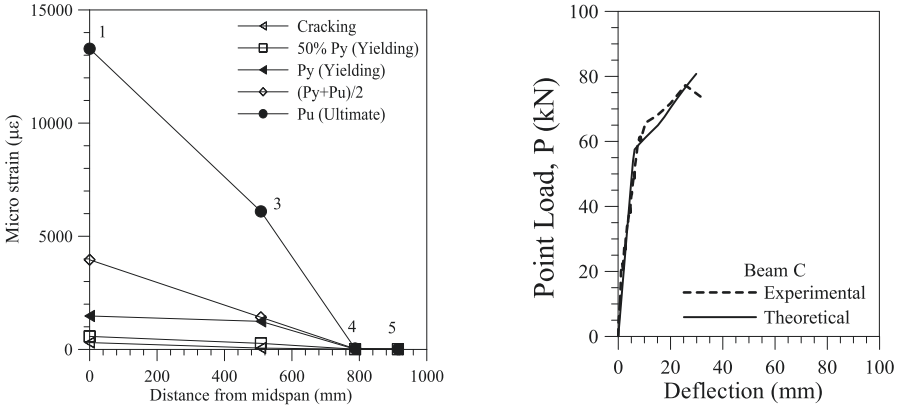

(a) Strain gage profiles **(b)** Load-Deflection curves of beam C

Fig. 13. Test results of beam C.

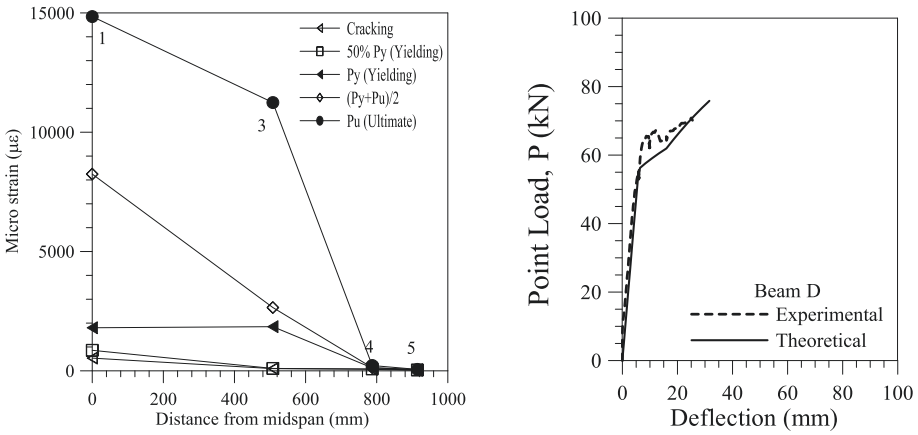

(a) Strain gage profiles **(b)** Load-Deflection curves of beam D

Fig. 15. Test results of beam D.

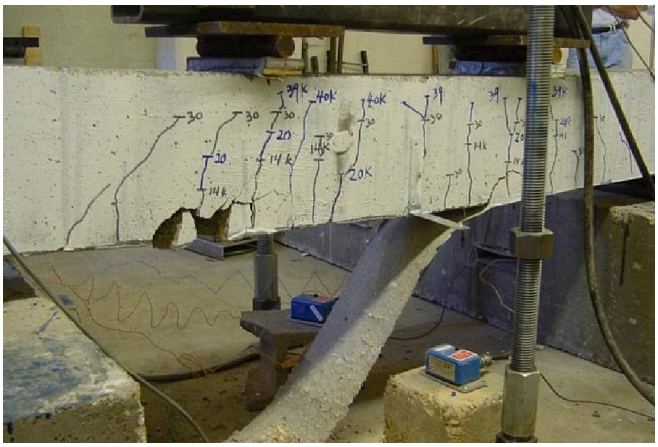

Fig. 16. Failure mode of beam E.

Since neither slippage of the grid from the polyurea during the coupon test nor debonding at any interface during the bending test of RC beams strengthened with GFRP grid reinforced polyurea was observed, the assumption that plain sections remain plain was used in developing the analytical model. Therefore, typical analysis of RC beams strengthened with FRP system reported in literature was applied in analyzing the beams from this study [11,15,20]. Moreover, theoretical analysis for flexural strength of RC beams strengthened with sprayed polyurea coating has been conducted by Greene and Myers [24] and Parniani and Toutanji [37].

The bending stiffness shown in Table 2 is calculated according to

$$EI = \frac{Pa}{24\Delta_u}(3L^2 - 4a^2) \tag{2}$$

Where a is the distance from the support to the point load, L is the clear span of the beam, and P is the point load as shown in Fig. 2. Table 2 shows generally the cracking and yielding loads of the strengthened beams are greater than those of the control beam. The bending stiffness and yielding load of Beam C is significantly higher than those of Beam B. However, in Beams C and B the cracking load is the same, which suggest addition of GFRP grid to the polyurea has negligible effects on the initial cracking of the strengthened beams. Research results also indicate that the cracking, yielding and ultimate loads of Beam E, which was strengthened with GFRP sheet, are higher than those of RC beams strengthened with GFRP grid no matter sprayed polyurea or polymer was used as bonding agency (Beams C and D). As the bending stiffness of Beam C is greater than that of Beam D, it is reasonable to conclude that the sprayed polyurea is more efficient in increasing the stiffness of RC beams. Moreover, since the ultimate load and ductility index (Table 2) of

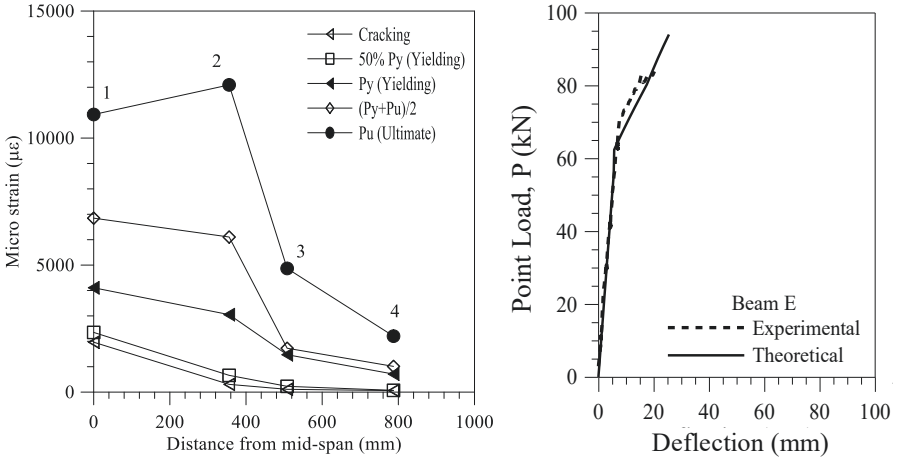

(a) Strain gage profiles **(b)** Load-Deflection curves of beam E

Fig. 17. Test results of beam E.

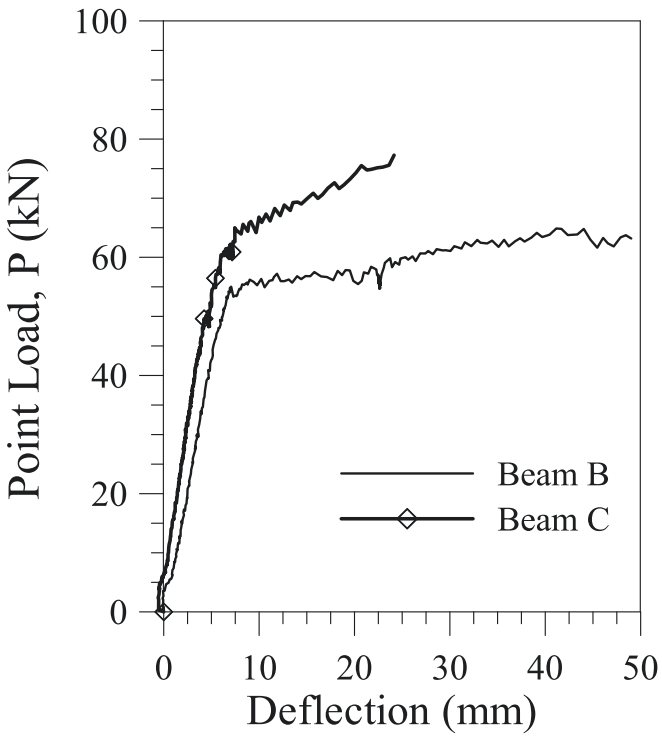

Fig. 18. Comparison of load–deflection curves for beams B and C.

Beam C are both greater than those of Beam D, sprayed polyurea would be an ideal bonding agency when GFRP grid is used for structural strengthening of RC beams.

5. Comparison with results from literature

Results from tensile test of fabric reinforced composites from open literature are compared in Table 3 and results from bending test of RC beams strengthened with polyurea or FRCM are included in Tables 4 and 5 for further analysis.

5.1. Impregnation of fabric to the mechanical properties of FRCM

It was reported [38,39] in Table 3 that for the same mortar the tensile strength and ultimate strain of FRCM reinforced with coated carbon were much greater than that of composite with dry carbon fabric recorded from the tensile test. The reason was that coating of the fabric with epoxy improved bond between the inner and outer filaments of each yarn and between yarns and matrix. As a result, slippage was postponed or prevented, and the coated fabric can then develop higher tensile stress and achieve a higher failure strain [17]. Therefore, coating or impregnation of fabric may change the failure mode from slippage to rupture of fabric and can clearly increase the tensile strength and ultimate strain of FRCM. It was reported that geometry of the fabric has an obvious effect on the mechanical properties of composites [10,12,13,31], therefore, the contribution of impregnation of fabric on the property of the FRCM needs to be further studied according to the geometry and material of the fabric, and others.

Table 3
Comparison of tensile test results of one-ply fabric reinforced composites at failure.

Resource	Specimen	Matrix material	Fabric material	Failure mode of composite	Strain of fabric[&] (a)	Strain of composite (b)	(b)/(a)
Caggegi et al. [9]	TT1_M1_3	Mortar	Basalt*	Rupture of fabric	0.02**	0.0106	0.53
	TT1_M1_4				0.02**	0.0128	0.64
	TT1_M1_5				0.02**	0.0157	0.785
Li et al. [12]	C-3–1-1	ECC	Basalt*	Rupture of fabric	0.0231	0.0155	0.67
	C-3–1-2				0.0231	0.0143	0.62
	C-3–1-4				0.0231	0.0150	0.65
	C-4–1-1				0.0231	0.0139	0.60
	C-4–1-2				0.0231	0.0111	0.48
	C-4–1-4				0.0231	0.0133	0.58
	C-6–1-1				0.0231	0.0151	0.65
	C-6–1-2				0.0231	0.0128	0.55
	C-6–1-3				0.0231	0.0189	0.82
Padalu et al.[40]	25 mm mesh	Mortar	Basalt#	Rupture of fabric	0.0196/	0.0156/	0.80/
	weft/warp				0.0187	0.0114	0.61
	50 mm mesh				0.0201/	0.0106/	0.53/
	weft/warp				0.0247	0.0134	0.54
Leone et al. [41]	#A(Polimi)	Mortar	Glass#	Rupture of fabric	0.03	0.0049	0.16
	#B-4(Units)		Glass*		0.015	0.0184	1.22
	#B-5				0.015	0.0108	0.72
	#C(Unibo)		Glass#		0.02	0.0154	0.77
	#C(Cut)				0.02	0.0175	0.88
	#E(Upatras)		Glass*		>0.03	0.0138	0.46
	#G(Polimi)				0.041	0.0123	0.30
Carozzi and Poggi [10]	PBO-1	Mortar	PBO#	Rupture of fabric	N/A	N/A	0.85
	G		Glass*		N/A	N/A	0.81
Younis et al. [42]	G-N1	Mortar	Glass*	Rupture of fabric	0.0325	0.0122	0.38
Donnini and Corinaldesi [38]	CM_C	Mortar	Carbon#	Slippage of fabric	0.02	0.0058	644(MPa)[$]
	CM_CC		Carbon*	Rupture of fabric	0.02	0.0226	1358(MPa)[$]
Raoof et al. [39]	Carbon	Mortar	Carbon#	Rupture of fabric	N/A	0.0079	1518(MPa)[$]
			Carbon*		N/A	0.0139	2843(MPa)[$]
This study	Specimen A	Polyurea	Glass*	Rupture of fabric	0.0180	0.0232	1.29
	Specimen B				0.0180	0.0243	1.35
	Specimen C				0.0180	0.0241	1.34

[*] Impregnated or coated with epoxy resin;
[&] Determined from tensile test or provided by the manufacturer in the resource;
[**] Approximated from figure of the resource by the authors of this paper;
[$] Tensile strength;
[#] Dry fabric.

Table 4
Bending test results of RC beams strengthened with polyurea system.

Resource	Beam	Thickness of polyurea (mm)	Volume ratio of glass fiber (%)	Ultimate strain of composite (%)	Elastic modulus of composite (GPa)	Tensile strength of composite (MPa)	Failure mode of beam	Failure load of beam P (kN)	Increase ΔP/P (%)
This study	A	–	–	–	–	–	CC**	64.5	–
	B	7	0	43.8	0.20	7	CC	67.4	4.5
	C	7	5.3*	2.3	2.00	39	Polyurea rupture	77.3	19.8
Greene and Myers [24]	1	6#	0	91	–	14.8	CC	138	23.8
	2	5.3#	3.0	13.3	0.28	6.9	CC	122	9.7
	3	5.6#	10.8	9.3	1.13	12.8	CC	129	15.4
	4	4.9#	7.2	13.2	0.66	9.7	CC	113	1.3
	5	–	–	–	–	–	CC	110	–
Parniani and Toutanji [37]	C-B-M	–	–	–	–	–	CC	29.4	–
	P-B-M−1	2.5	0	700	N/A	15.8	CC	32.1	9.2
	P-B-M−2	5.0	0	700	N/A	15.8	CC	34.5	17.3
Song and Eun [25]	N-F	–	–	–	–	–	CC	60.69	–
	PO-F-A	5.0	0	–	–	14	CC	67.51	11
	PG-F-A	5.0	5.0$	–	–	16	CC	65.41	8.0

* In the direction of tensile load;
** Concrete crushing after yielding of tensile steel reinforcement;
\# Approximated from figure of the resource by the authors of this paper;
$ Weight ratio.

5.2. Comparison of polyurea versus inorganic matrix in properties of composites in tensile test

Table 3 shows that the rupture strain of FRCM in the tensile test was lower than that of the fabric itself no matter the fabric was coated or impregnated or not. Even with a small addition of polymer mortar is brittle with ultimate tensile strain of around 0.5% and ECC is more ductile with the recorded fracture strain up to 7% [12], no significant difference of strain reduction ratio (mainly in the range of 0.3–0.8) was observed when basalt, carbon, glass or PBO fabric was used as the reinforcement. The reason is that the in-organic matrix was not effective enough to prevent stress concentration even to the impregnated grid. On the contrary, Table 3 shows that fracture strain of the GFRP grid embedded in polyurea was much greater than that of plain FRP grid due to the excellent mechanical properites of the polyurea (high elastic limit and high strength). Therefore, the sprayed polyurea is superior to cement based matrix in terms of preventing premature rupture and achieving the full strain potential of the grid reinforcement.

5.3. Effectiveness of polyurea to flexural strengthening of RC beams

Table 4 shows that the flexural strength of RC beams strengthened with plain polyurea coating increased significantly. It seems that simply increasing the thickness of the polyurea did not change the failure mode of the beam. For all beams in Table 4, no debonding of the polyurea system was observed, which means ideal bond strength existed between the concrete members and polyurea system. Therefore, due to the high tensile strength and bond strength, sprayed polyurea alone could be an effective scheme for flexural strengthening of RC beams. Moreover, compared with strengthening with discrete fiber reinforced polyurea [24,25], when similar amount of fiber material is used, application with fiber grid reinforced polyurea achieved greater gain of flexural capacity and proved to be more efficient and reliable. Meanwhile, the thickness of the polyurea system was smaller than the nominal thickness of FRCM, which was typically 8–10 mm, as specified in ACI 549 [31].

5.4. Impregnation of fabric to strengthening efficiency of RC beams

It is depicted in Tables 2 and 5 that for strengthening of RC beams with impregnated FRP grid reinforced composite, when the beams failed due to rupture of the grid at mid-span, comparable strengthening efficiency of $\Delta P_u/(A_f E_f)$ was achieved by GFRP grid reinforced polyurea (Beam C in Table 2) and BFRP grid reinforced ECC (Beams BCBS1, BCBS4 and BCBS7 in Table 5). Meanwhile, a much higher $\Delta P_u/(A_f E_f)$ was reached by strengthening of RC beams with impregnated CFRP grid bonded with ECC, epoxy or PCM (see the test results reported by Yang et al. [19] and Guo et al. [20] in Table 5). Therefore, strengthening of RC beams with impregnated FRP grid with higher axial stiffness or tensile strength may achieve a greater increase of flexural capacity even when different matrix were employed. This agrees with the finding that more gain of flexural capacity was achieved for RC beams strengthened with FRCM with higher axial stiffness of fabric during the bending test [11].

As for Beams II series and III series by Yang et al. [19] in Table 5, the only difference was the bonding matrix and the ultimate strain of the grid was very close when the beams failed due to rupture of grid. This means that when cement based matrix with high ductility was used as bonding agency, the area of grid required for the same increase of flexural strength of RC beams can be the same as that for polymer matrix. This is different from strengthening of RC beams with dry textile reinforced matrix, where it is reported that when the same amount of textile was used, the strengthening effect for textile bonded with inorganic matrix was half of that with organic matrix as the interfacial bond strength between the textile and cement matrix was weaker than that between textile and polymer [5]. Meanwhile, it is reported by Raoof et al. [39] that for flexural strengthening of RC beams with FRCM, application of coated carbon fabric achieved greater increase of flexural strength when compared with dry carbon fabric (see Table 5). Since impregnation of dry fabric clearly increased the mechanical performance of the FRCM and the strengthening efficiency of RC beams, when cement-based matrix is used as bonding agency, it is beneficial to use impregnated fabric.

5.5. Effectiveness of additional end anchorage of fabric or grid system

It was reported that providing end anchorage had a limited effect on the performance of TRM-retrofitted beams [39]. For strengthening of RC beams with FRCM, debonding or slippage is likely to happen even when additional U-wrap anchorage is employed. Because of the poor bonding

Table 5
Comparison with results of RC beams from 4 point bending test from literature.

Resource	Specimen	End-anchorage	Grid type	Matrix type	Failure mode	P_u (kN)	A_fE_f (kN)	$\frac{\Delta P_u}{A_fE_f}$	ε_u ($\mu\varepsilon$)	ε_{exp} ($\mu\varepsilon$)	$\frac{\varepsilon_{exp}}{\varepsilon_u}$
Yang et al. [19][1]	I-10 [3]	–	–	–	Crushing of concrete	51.9	–	–	–	–	–
	II-10	U-wrap	CFRP	ECC	Debonding and rupture of grid near the end	95.5	1320	0.033	14,000	12,780	0.91
	II-12	U-wrap	CFRP	ECC	Debonding and rupture of grid near the end	104.8	1320	0.040	14,000	10,536	0.75
	II-16	U-wrap	CFRP	ECC	Rupture of grid at mid-span	126.8	1320	0.057	14,000	7513	0.54
	III-10	U-wrap	CFRP	Epoxy	Partial separation and grid rupture	89.3	1320	0.028	14,000	13,440	0.96
	III-12	U-wrap	CFRP	Epoxy	Partial separation and grid rupture	105.5	1320	0.041	14,000	11,099	0.79
	III-16	U-wrap	CFRP	Epoxy	Grid rupture at mid-span	129.3	1320	0.059	14,000	7928	0.57
Zheng et al. [18][1]	CL [3]	–	–	–	Crushing of concrete	126	–	–	–	–	–
	BBB-1–500	None	BFRP	ECC	Rupture of FRP grid	131	N/A	N/A	7000 [4]	1300 [4]	0.19
	BBB-3–500	None	BFRP	ECC	Rupture of FRP grid	146	N/A	N/A	7280 [4]	5600 [4]	0.80
	BBB-5–500	None	BFRP	ECC	Partial debonding after rupture of FRP grid	167	N/A	N/A	7300 [4]	5500 [4]	0.75
	BBB-3–450	None	BFRP	ECC	Rupture of FRP grid	141	NA	NA	7280 [4]	6000 [4]	0.82
	BBB-3–400	None	BFRP	ECC	Rupture of FRP grid	136	NA	NA	7280 [4]	6300 [4]	0.87
Guo et al. [20][1]	NR [3]	–	–	–	Crushing of concrete	55.4	–	–	–	–	–
	ROH	None	CFRP	PCM	CFRP grid debonding	202	44,720	0.0033	7970 [4]	5380	0.675
	ROL	None	CFRP	PCM	CFRP grid rupture	186	14,000	0.0093	8415 [4]	8275	0.983
	RTH	None	CFRP	PCM	CFRP grid debonding	207	29,322	0.0052	7230 [4]	5389	0.745
	RTL	None	CFRP	PCM	CFRP grid rupture	169	11,194	0.0101	8387 [4]	8824	1.052
Zheng et al. [21][1]	BCS4[3]	–	–	–	concrete crushing	101.4	–	–	–	–	–
	BCBS1	None	BFRP	ECC	Rupture of grid + concrete crushing	106.5	1675.8 [4]	0.0030	21,600	14,473	0.67
	BCBS2	None	BFRP	ECC	Concrete crushing	117.7	4858.4 [4]	0.0034	20,800	11,676	0.56
	BCBS3	None	BFRP	ECC	Concrete crushing	126.3	8121.8 [4]	0.0031	21,400	15,906	0.74
	BCCS1	None	CFRP	ECC	Concrete crushing	137.4	12693.5 [4]	0.0026	16,400	6427	0.40
	BCS2[3]	–	–	–	Concrete crushing	94.6	–	–	–	–	–
	BCBS4	None	BFRP	ECC	Rupture of grid + concrete crushing	101.4	1756.7 [4]	0.0039	21,600	10,733	0.50
	BCCS2	None	CFRP	ECC	Concrete crushing	125.7	7857.2 [4]	0.0040	16,200	7376	0.45
	BCCS3	None	CFRP	ECC	Concrete crushing	153.4	13347.6 [4]	0.0044	16,400	8147	0.50
	BCCS4	None	CFRP	ECC	Concrete crushing	132.3	18624.9 [4]	0.0020	16,000	5478	0.34
	BCS5[3]	–	–	–	Concrete crushin	89.3	–	–	–	–	–
	BCBS7	None	BFRP	ECC	Rupture of grid + concrete crushing	96.4	1844.9 [4]	0.0039	21,600	12,422	0.58
	BCBS8	None	BFRP	ECC	Concrete crushing	108.7	5387.6 [4]	0.0037	20,800	14,294	0.66
	BCBS9	None	BFRP	ECC	Concrete crushing	113.0	8937.6 [4]	0.0027	21,400	12,254	0.56
	BCCS5	None	CFRP	ECC	Concrete crushing	144.7	14009.1 [4]	0.0029	16,400	7908	0.49
Elghazy et al. [8][2]	CU [3]	None	None	None	–	72.2	–	–	–	–	–
	CRS-4P-I	U-wrap	PBO	Cement matrix	FRCM delamination	102.8	3630 [4]	0.0084	14,000[5]	8446	0.60
	CRS-4P-II	U-wrap	PBO	Cement matrix	Extensive fabric slippage	111.1	3630 [4]	0.0107	14,000[5]	9653	0.69
	CRS-3C-II	U-wrap	CFRP	Cement matrix	Extensive fabric slippage	109.3	5203 [4]	0.0071	12,500[5]	9777	0.78
	CRL-4P-I	U-wrap	PBO	Cement matrix	FRCM delamination	91.1	3630 [4]	0.0052	14,000[5]	7409	0.53
	CRL-4P-II	U-wrap	PBO	Cement matrix	Partial debonding of the fabric	108.1	3630 [4]	0.0099	14,000[5]	8928	0.64
	CRL-3C-II	U-wrap	CFRP	Cement matrix	Extensive fabric slippage	131.9	5203 [4]	0.0115	12,500[5]	13,876	1.11
Raoof et al. [39]	CON[3]	–	–	–	–	34.6	–	–	–	–	–
	M1_C[2]	None	Carbon	Cement matrix	Slippage and partial rupture	39.0	N/A	N/A	N/A	N/A	0.90[6]
	M1_CCo[1]	None	Coated Carbon	Cement matrix	Debonding at the fabric-mortar interface	41.3	N/A	N/A	N/A	N/A	0.64[6]

ε_u:ultimate strain from coupon test or provided by manufacturer; ε_{exp}:experimental strain of FRP system at mid-span of RC beams at failure;
[1] flexural strengthened with impregnated FRP grid reinforced matrix;
[2] flexural strengthened with dry fabric or textile reinforced matrix;
[3] control beam without strengthening;
[4] values not provided and were computed or approximated with information from original resource by the authors of this paper;
[5] values were determined through tensile test of FRCM coupons;

[6] values are ratio of the maximum stress of FRCM from beam test divided by the tensile strength determined from the tensile test of coupons.

between fabric and cement-based matrix, even the debonding was prevented due to the additional end anchorage, slippage of fabric may occur (see results by Elghazy et al. [8] in Table 5). Meanwhile, Table 5 shows that for the test by Yang et al.[19] after end U-wrap was applied, even the beams did not fully fail due to rupture of the grid, the beams strengthened with impregnated CFRP grid reinforced ECC(II-10,II-12,II-16) achieved nearly the same strengthening efficiency as beams with epoxy counterpart (III-10,III-12,III-16). Therefore, in order to increase strengthening efficiency, additional bonding measurement is recommended for strengthening of RC beams with impregnated FRP grid when cement-based mortar is used.

5.6. Strain of FRP grid system used in strengthening of RC beams

It is indicated in Tables 1 and 5 that most beams failed due to rupture of the grid system and the maximum recorded strain for the composite was 30–90% of the ultimate strain determined through direct tensile tests. Therefore, even impregnation of fabric with epoxy resin helped to improve bonding of yarn with matrix and distribute tensile load more evenly [17], reduction of the failure strain of the grid system has to be adopted.

Tables 3 and 5 show that the recorded rupture strain of the grid reinforced composites varied significantly and is related to the ultimate strain of the grid. ACI 549.4R [31] regulates the limit for effective strain of the FRCM as 0.012. Table 3 shows that the rupture strain of most fabric, especially the impregnated grid, was much greater than 0.012 during the tensile test. The effective strain of 0.012 is justifiable for the beams strengthened with low rupture strain grid during the bending test, but it clearly underestimates the strain of FRP system when grid with higher ultimate strain is used, as shown from the results by Yang et al.[19] and Zheng et al.[21] in Table 5. Therefore, the effective strain of FRCM should be modified according to the material of fabric and bonding agency. Furthermore, 0.012 is much lower than the recorded rupture strain of the GFRP grid reinforced polyurea as shown in Tables 1 and 3.

6. Conclusions

This study investigated the mechanical properties of polyurea system and flexural strengthening of RC beams with GFRP grid bonded with sprayed polyurea and the following conclusions could be drawn from this research:

No slippage of GFRP grid or distributed cracks of the polyurea was observed and the full strength and ultimate strain of GFRP grid were achieved during the tensile test of GFRP grid reinforced polyurea. Comparison with test results of other composites from open literature shows that polyurea performed better than other inorganic materials when used as matrix for fabric during the tensile test.

Strengthening of RC beams with polyurea not only increased the flexural capacity but also improved the serviceability of the beams by reducing the crack width and decreasing the mid-span deflection. Compared with other strengthening schemes, flexural strengthening with GFRP grid bonded with polyurea demonstrated to be effective with many advantages, including significantly less time required for curing and satisfactory bonding performance of polyurea system to RC beams.

In order to achieve the same increase of flexural strength of RC beams, the amount of impregnated grid required for the cement based matrix could be the same as that for organic matrix. When cement based matrix is used as bonding agency, it is beneficial to impregnate fabric with epoxy resin before application.

For most beams flexural strengthened with FRP grid system the recorded strain of grid was 30–90% of the ultimate strain determined from coupon test when the beams failed due to rupture of the grid. The strain limit of 0.012 by ACI 549 [31] is justifiable for grid with relatively low rupture strain, but underestimates the failure strain of FRCM with impregnated grid or matrix with high ultimate strain. The experimental ultimate strain of GFRP grid reinforced polyurea was much greater than 0.012.

Future areas that warrant further research can be highlighted as follows: (1) confinement effects of polyurea systems in increasing the confinement strength of RC members under axial loads [43]; (2) effects of loading schemes and bond strength of grid reinforced polyurea to concrete in delaying intermediate crack (IC) debonding failure and cover delamination of RC beams during the flexural testing;, (3) response of grid reinforced polyurea strengthened RC members under dynamic loads such as fatigue, earthquake, and among many other high impulse loads.

CRediT authorship contribution statement

Piyong Yu: Investigation, Data curation, Formal analysis, Writing – original draft. **Pedro Silva:** Methodology, Software, Formal analysis, Writing – review & editing. **Antonio Nanni:** Conceptualization, Writing – review & editing, Supervision.

Declaration of Competing Interest

The authors declare that they have no known competing financial interests or personal relationships that could have appeared to influence the work reported in this paper.

Data availability

Data will be made available on request.

References

[1] ACI Committee 440. 2017. Guide for the Design and Construction of Externally Bonded FRP Systems for Strengthening Concrete Structures (ACI 440.2R-17), Farmington Hills, Michigan.
[2] Alkhrdaji T, Nanni A, Chen G, Barker M. “Upgrading the Transportation Infrastructure: Solid RC Decks Strengthened with FRP”. *Concrete International: Design and Construction* 1999;21(10):37–41.
[3] Bakis CE, Bank LC, Brown VL, Cosenza E. Fiber-Reinforced Polymer Composites for Construction—State-of-the-Art Review. J Compos Constr 2002;6(2):73–87.
[4] Teng JG, Chen JF, Smith ST, Lan L. FRP-strengthened RC structures. New York: Wiley; 2002.
[5] Orosz K, Blanksvard T, Taljsten B, Fischer G. From material level to structural use of mineral-based composites-An overview. Advances in Civil Engineering 2010. Article ID:985843.
[6] Bencardino F, Carloni C, Condello A, Focacci F, Napoli A, Realfonzo R. Flexural behavior of RC members strengthened with FRCM: State of the art and predictive formulas. Compos B Eng 2018.
[7] Elsanadedy HM, Almusallam TH, Alsayed SH, Al-Salloum YA. Flexural strengthening of RC beams using textile reinforced mortar-experimental and numerical study. Compos Struct 2013;97:40–55.
[8] Elghazy M, Refai AE, Ebead U, Nanni A. Post-repair flexural performance of corrosion-damaged beams rehabilitated with fabric-reinforced cementitious matrix (FRCM). Construct Build Mater 2018;166:732–44.
[9] Caggegi C, Lanoye E, Djama K, Bassil A, Gabor A. Tensile behaviour of a basalt TRM strengthening system: Influence of mortar and reinforcing textile ratios. Compos B Eng 2017. https://doi.org/10.1016/j.compositesb.2017.07.027.
[10] Carozzi FG, Poggi C. Mechanical properties and debonding strength of fabric reinforced cementitious matrix (FRCM) systems for masonry strengthening. Compos B Eng 2015;70:215–30.
[11] Ebead U, Shrestha KC, Afzal MS, Refai AE, Nanni A. Effectiveness of fabric-reinforced cementitious matrix in strengthening reinforced concrete beams. J Compos Constr 2016;04016084.
[12] Li BB, Xiong HH, Jiang JJ, Dou XX. Tensile behavior of basalt grid reinforced engineering cementitious composites. Compos B Eng 2019;156:185–200.
[13] Peled A, Bentur A. Fabric structure and its reinforcing efficiency in textile reinforced cement composites. Compos A 2003;34:107–18.
[14] D’Ambrisi A, Focacci F. Flexural strengthening of RC beams with cement-based composites. J Compos Constr 2011;15(5):707–20. https://doi.org/10.1061/(ASCE)CC.1943-5614.0000218.

[15] Babaeidaradad S, Loreto G, Nanni A. Flexural strengthening of RC beams with an externally bonded fabric-reinforced cementitious matrix. J Compos Constr 2014;18 (5):04014009. https://doi.org/10.1061/(ASCE)CC.1943-5614.0000473.
[16] Homoro O, Michel M, Baranger TN. Pull-out response of glass yarn from ettringite matrix: Effect of pre-impregnation and embedded length. Compos Sci Technol 2019;170:174–82.
[17] Donnini JV, Corinaldesi V, Nanni A. Mechanical properties of FRCM using carbon fabrics with different coating treatments. Compos B Eng 2016;88:220–8.
[18] Zheng YZ, Wang WW, Brigham JC. Flexural behavior of reinforced concrete beams strengthened with a composite reinforcement layer: BFRP grid and ECC. Construct Build Mater 2016;115:424–37. https://doi.org/10.1016/j.conbuildmat.2016.04.038.
[19] Yang X, Gao WY, Dai JG, Lu ZD, Yu KQ. Flexural strengthening of RC beams with CFRP grid-reinforced ECC matrix. Compos Struct 2018;108:9–26. https://doi.org/10.1016/j.compstruct.2018.01.048.
[20] Guo R, Hu WH, Li MQ, Wang B. Study on the flexural strengthening effect of RC beam reinforced by FRP grid with PCM shotcrete. Compos Struct 2020.
[21] Zheng AH, Liu ZZ, Li FP, Li S. Experimental investigation of corrosion-damaged RC beams strengthened in flexure with FRP grid-reinforced ECC matrix composites. Eng Struct 2021;244:112779.
[22] Chris G. Polyurea: a market overview. Eur Coat J 2000;October:54.
[23] Shojaei B, Najafi M, Yazdanbakhsh A, Abtahi M, Zhang CW. A review on the applications of polyurea in the construction industry. Polym Adv Technol 2021; 1–16.
[24] Greene CE, Myers JJ. Flexural and shear behavior of reinforced concrete members strengthened with a discrete fiber-reinforced polyurea system. J Compos Constr 2013;17:108–16.
[25] Song JH, Eun HC. Improvement of flexural and shear strength of RC beam reinforced by glass fiber-reinforced polyurea (GFRPU). Civil Engineering Journal 2021;3(7):407–18.
[26] Rizwan M, Khaleequzzaman S, Zaman UKU. Tensile Strength Improvement of Concrete Slabs Using Polyurea Spray. Pract Period Struct Des Constr 2021;26(1): 04020048.
[27] ASTM D3039/D3039M.2014. Standard test method for tensile properties of polymer matrix composite Materials.
[28] Zeng Y, Caspeele R, Taerwe L. Compressive membrane action in FRP-strengthened concrete beams. Elegance in Structures IABSE Conference Nara 2015:5.
[29] ACI Committee 546.2014. Guide to Concrete Repair (ACI 546R-14), American Concrete Institute, Farmington Hills, Michigan. 70 pp.
[30] International Concrete Repair Institute, ICRI. 2013. Selecting and Specifying Concrete Surface Preparation for Sealers, Coatings, Polymer Overlays, and Concrete Repair, ICRI 310.2R-2013, St. Paul, Minnesota, 48 pp.
[31] ACI Committee 549.4R. 2013. Guide to Design and Construction of Externally Bonded Fabric-reinforced Cementitious Matrix (FRCM) Systems for Repair and Strengthening Concrete and Masonry Structures (ACI 549.4R-13), American Concrete Institute, Farmington Hill, Michigan.
[32] Caggegi C, Carozzi FG, Santis SD, et al. Experimental analysis on tensile and bond properties of PBO and aramid fabric reinforced cementitious matrix for strengthening masonry structures. Compos B Eng 2017;15:175–95. https://doi.org/10.1016/j.compositesb.2017.05.048.
[33] Yu PY, Silva PF, Nanni A. Flexural strength of reinforced concrete beams strengthened with prestressed carbon fiber-reinforced polymer sheets—part II. ACI Struct J 2008.
[34] ACI Committee 318. 2019. Building Code Requirements for Structural Concrete (ACI 318-19) and Commentary (ACI 318R-19), American Concrete Institute, Farmington Hills, Michigan.
[35] Zhang SS, Ke Y, Chen E, Biscaia H, Li WG. Effect of load distribution on the behaviour of RC beams strengthened in flexure with near-surface mounted (NSM) FRP. Compos Struct 2022;279:114782.
[36] Kang THK, Howell J, Kim S, et al. A State-of-the-Art Review on Debonding Failures of FRP Laminates Externally Adhered to Concrete. Int J Concr Struct Mater 2012;6: 123–34. https://doi.org/10.1007/s40069-012-0012-1.
[37] Parniani S, Toutanji H. Monotonic and fatigue performance of RC beams strengthened with a polyurea coating system. Construct Build Mater 2015;101: 22–9.
[38] Donnini JV, Corinaldesi V. Mechanical characterization of different FRCM systems for structural Reinforcement. Construct Build Mater 2017;145:565–75.
[39] Raoof SM, Koutas LN, Bournas DA. Textile-reinforced mortar (TRM) versus fibre-reinforced polymers (FRP) in flexural strengthening of RC beams. Construct Build Mater 2017;151:279–91.
[40] Padalua PKVR, Singh Y, Das Y. Efficacy of basalt fibre reinforced cement mortar composite for out-of-plane strengthening of unreinforced masonry. Construct Build Mater 2018;191:1172–90.
[41] Leone M, Aiello MA, et al. Glass fabric reinforced cementitious matrix: Tensile properties and bond performance on masonry substrate. Compos B Eng 2017;127: 196–214.
[42] Younis A, Ebead U, Shrestha K. Tensile Characterization of multi-ply fabric-reinforced cementitious matrix strengthening systems. Struct Concr 2019;1–11.
[43] Tang Z, Li WG, Tam VWY, Yan L. Mechanical performance of CFRP-confined sustainable geopolymeric recycled concrete under axial compression. Eng Struct 2020;224:111246.